LEGIBILITY NOTICE

A major purpose of the Technical Information Center is to provide the broadest dissemination possible of information contained in DOE's Research and Development Reports to business, industry, the academic community, and federal, state and local governments.

Although a small portion of this report is not reproducible, it is being made available to expedite the availability of information on the research discussed herein.

Los Alamos National Laboratory is operated by the University of California for the United States Department of Energy under contract W-7405-ENG-36

LA-UR--89-669

DE90 007506

TITLE: Time Resolved Gain/Loss Studies Under Low and High Power Loading for the XeF C-A Transition

AUTHOR(S): Robert C. Sze, CLS-5

Marc Sentis, Institut de Mecanique des Fluides de Marseille CNRS, Marseille, France

Matteo Vannini, Istituto di Elettronica Quantistica del CNR Firenze, Italy

SUBMITTED TO: SPIE Proceedings of the International Congress on Optical Science and Engineering
March 12-16, 1990
The Hague, Netherlands

Time Resolved Gain/Loss Studies Under Low and High Power Loading for the XeF C-A Transition

Robert C. Sze
Los Alamos National Laboratory
Los Alamos, New Mexico 87545

Marc Sentis
Institut de Mécanique des Fluides de Marseille
CNRS
1 rue Honnorat
13003 Marseille, France

Matteo Vannini
Istituto di Elettronica Quantistica del CNR
Via Panciatichi 56/30
50127 Firenze, Italy

Abstract

The behavior of gain versus peak power deposition and the gain-length product versus total energy deposited are measured for devices with power deposition levels from 1 to 13 MW/cm^3 under a variety of gas mixtures. The temporal correlation between the power deposition and gain shows that both the fluorescence and the gain occur after the power deposition has concluded for excitation pulses in the range of 10-30 ns. We find that both B-X and C-A fluorescence takes place in the afterglow and their temporal shapes are similar. This indicates that the C and B states are tightly coupled. This tight coupling has two detrimental consequences for C-state lasing. First is that the population of the B and C states are approximately equal rather than 90 % in the C state believed to exist for short pulse electron beam excitation. We believe this close coupling is due to the presence of electric fields in the afterglow which keep the electron temperature relatively hot. The relative populations of the B and C states are determined by a Boltzman distribution governed by the electron temperature and their relative energy separation. Second is that with the C state lifetime approximately the same as the B state lifetime the C-A saturation intensity is very high and efficient energy extraction is substantially more difficult.

Introduction

Y. Nachshon, et al.[1] and Nighen, et al.[2] have shown that strong laser action in the C-A transition of XeF, despite its very large bandwidth, is possible under intense pumping with a short-pulse electron beam. This result has encouraged a flurry of activity to duplicate similar results in avalanche discharge devices[3-5]. The results, however, have not been encouraging. This paper deals with the correlation between gain and power deposition, and compares the temporal development of B and C state populations to explain why C-A lasing is so much poorer in avalanche discharges then in electron beam pumped systems.

Experimental Results

Data are taken on two modified Lumonics lasers in order to encompass a wide range of excitation conditions. A Lumonics TE292-K laser which is capable of delivering .5 J per pulse in the B-X transition of XeF in a 3 cm x 3 cm area beam of excellent uniformity is used to obtain gain and fluorescence characteristics in the blue-green C-A transition of XeF at power deposition levels measured in the region of 1 Mw/cm^3 and a pulse width of 30 ns. A Lumonics TE860 laser was modified to be able to accept from two to six rows of peaking capacitors as shown in Fig.1.

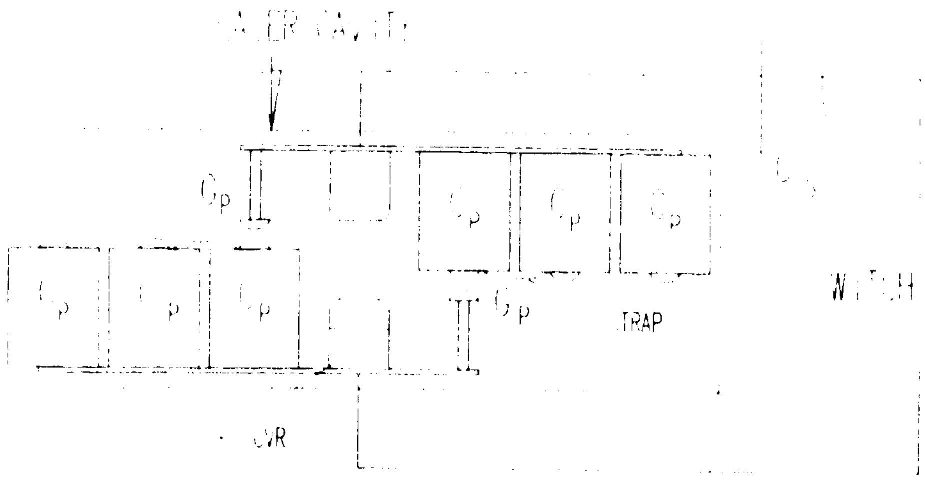

Figure 1. Laser cavity structure. C_s is the storage capacitor, C_p is the peaking capacitors, G_p is the gap for arc-type preionization, and CVR is a built in current viewing resister. Each row of peaking capacitors is made up of 15 capacitors of 0.5 nF each with an overall value of 7.5 nF. C_s = 30 or 60 nF.

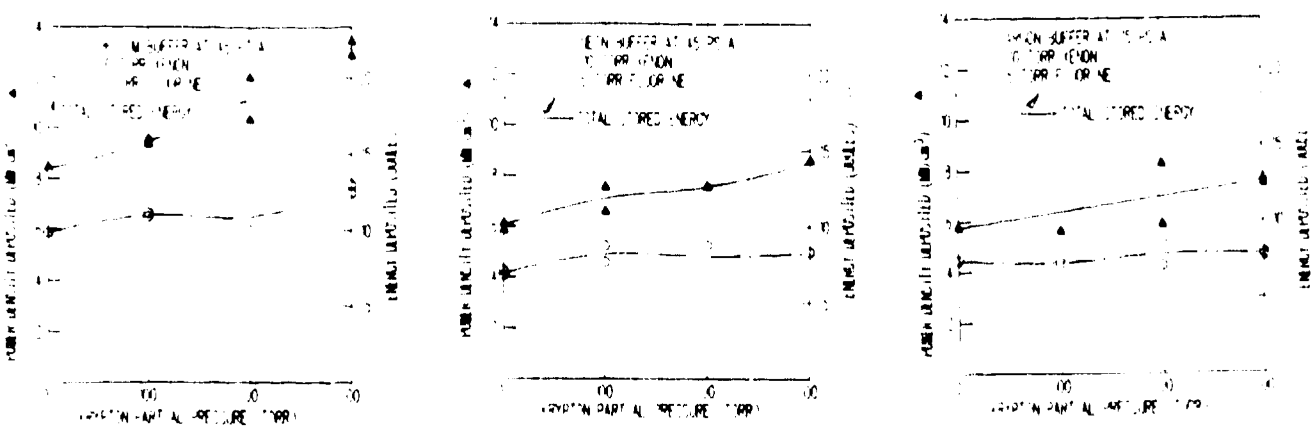

Figure 2. Peak-power deposition density and total energy deposited in the gas as a function of partial krypton pressure and are given with 10 torr xenon and 5 torr fluorine partial pressures at 45 psia total pressure in (a) helium and (b) neon buffers and at 15 psia total in (c) argon buffer. The storage capacitance C_s = 30 nF, the peaking capacitance C_p = 15 nF (two rows) and the charging voltage is 35 kV.

The measured peak power deposition density ranged between 6 to 13 MW/cm^3 and a deposition pulse width of 10 or 20 ns. We found that doubling the rows of peaking capacitors did not significantly increase the peak power deposition but mainly lengthened the deposition time. Figures 2 and 3 shows the peak power deposition density and the total energy deposited into the discharge for the cases of 2 rows and 4 rows of peaking capacitors respectively in different buffers as a function of increasing krypton pressure. The corresponding gain and gain-length product results for the same conditions for two and four rows of capacitors are presented in Figs. 4 and 5 respectively. Figure 6 gives the gain and gain-length products for the same gas mixtures and buffer gases under weak excitation in the 1 Mw/cm^3 level. We see from these results the peak gain is not proportional to the peak power deposition

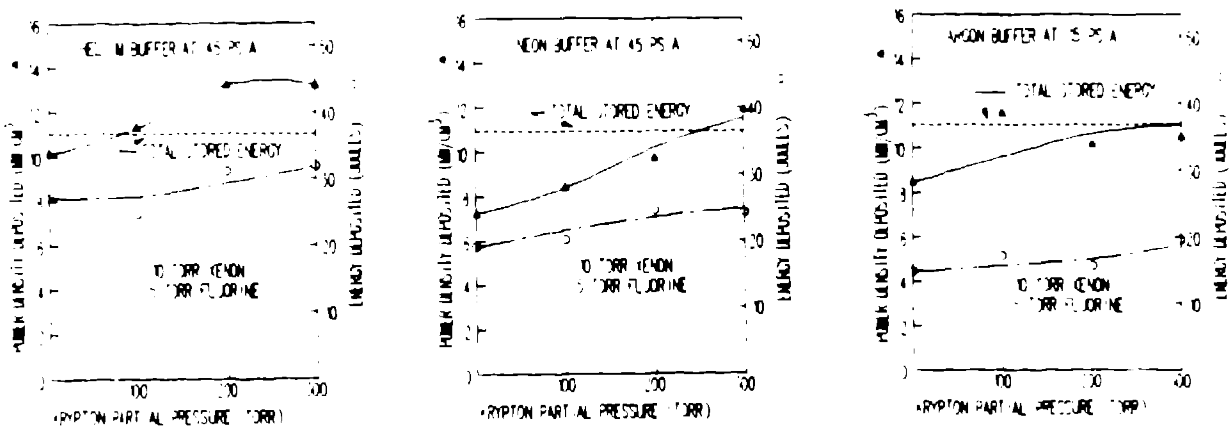

Figure 3. Same as Fig. 2 with storage capacitance C_s = 60 nF, the peaking capacitance C_p = 30 nF (four rows) and charging voltage of 35 kV.

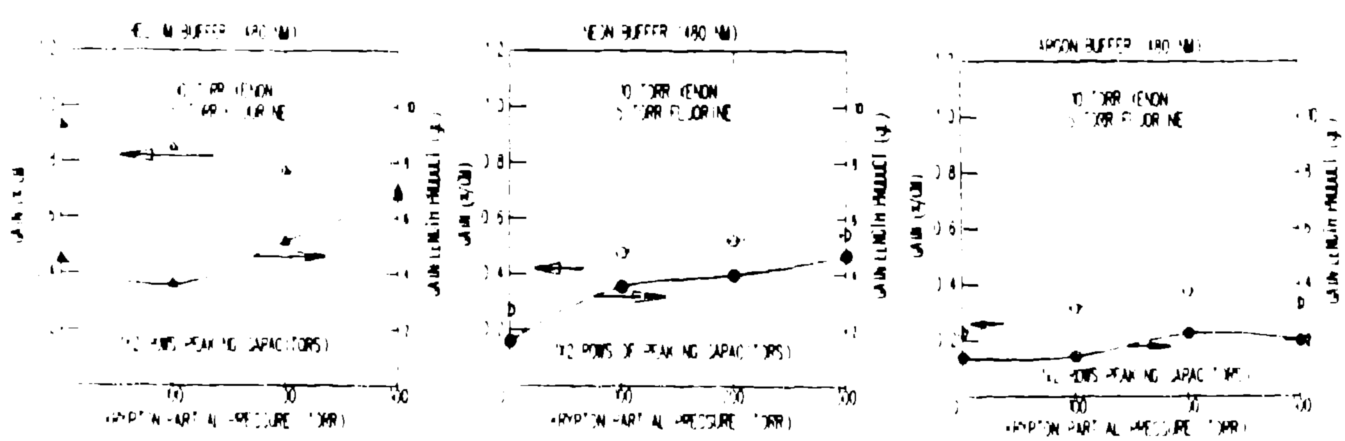

Figure 4. Peak gain and gain-length product versus changing krypton partial pressures in helium, neon, and argon buffers. Data are taken at 480 nm with device delivering peak powers between 6 to 13 MW/cm^3. C_s = 60 nF, C_p = 15 nF (two rows) and charging voltage of 35 kV.

for the situation where increased peak power deposition is accomplished by increasing the impedance of the discharge through increase in krypton partial pressure. If we look at the temporal evolution of the current, B-X fluorescence, C-A fluorescence and the C-A gain (shown in Fig.7 for two different krypton partial pressures), we see that both C-A and B-X fluorescence and gain takes place after the current pulse. During the discharge excitation we measure loss at the C-A transition wavelengths. Note that the B-X fluorescence is superradient in the absence of krypton and shows a narrower temporal width than the C-A transition. The temporal evolution of power deposition and gain are compared under high energy loading in Fig. 8. Gain exists only in the afterglow of the power deposition.

Figure 9 plots the gain (a) and gain-length product (b) as a function of peak power deposition and total energy deposited respectively for a gas mixture without

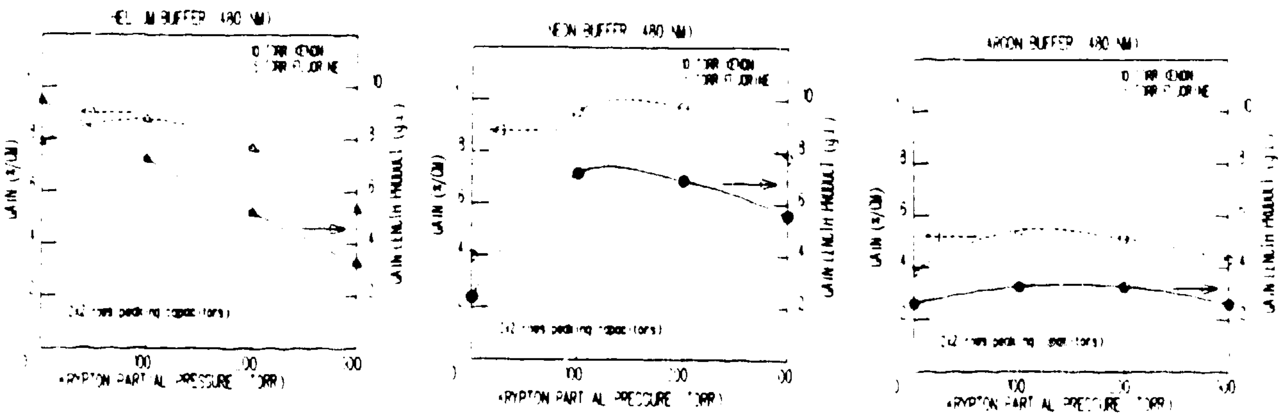

Figure 5. Same as Fig. 4 but with C_p = 30 nF (four rows).

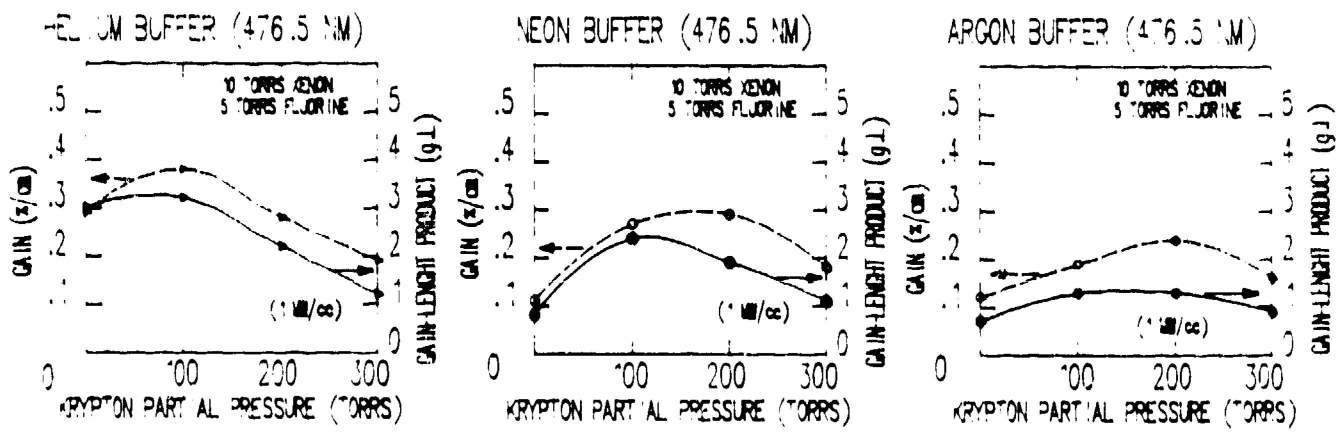

Figure 6. Peak gain and gain-length product versus changing krypton partial pressures in argon, neon, and helium buffers. Data are taken at 476.5 nm with device giving power deposition densities in the 1 MW/cm^3 level.

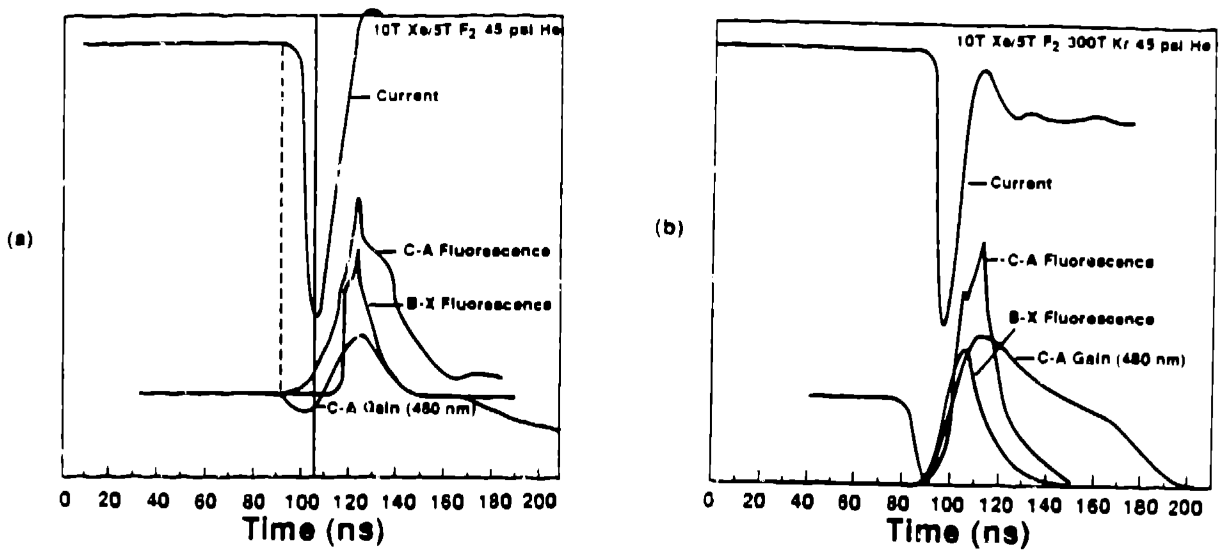

Figure 7. Temporal waveforms of current, C-A and B-X fluorescence, and C-A gain with total peaking capacitance C_p = 15 nF (two rows) and storage capacitance C_s = 30 nF. Time is in units of nanoseconds. The gas mixtures are for 45 psia total pressure in helium buffer with 10 torr xenon and 5 torr fluorine partial pressures and for (a) 0 torr krypton pressure and (b) 300 torr krypton pressure.

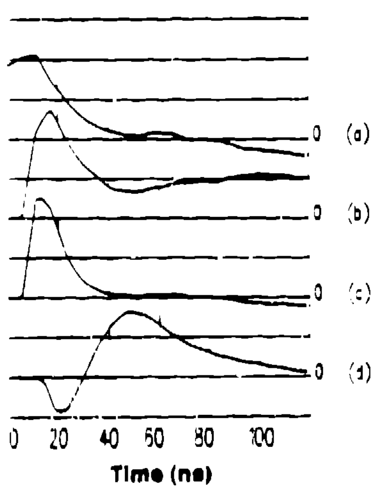

Figure 8. Temporal characteristics of (a) voltage (12.4kV/div), (b) current (16.5 kA/div), (c) power deposition (4 MW/cm^3/div) and (d) C-A gain (0.9%/cm/div) with total peaking capacitance C_p = 30 nF (four rows) and storage capacitance C_s = 60 nF. Time is in units of nanoseconds. The gas mixture is 45 psia total pressure in helium buffer with 0 torr krypton, 10 torr xenon, and 2 torr NF_3 partial pressures.

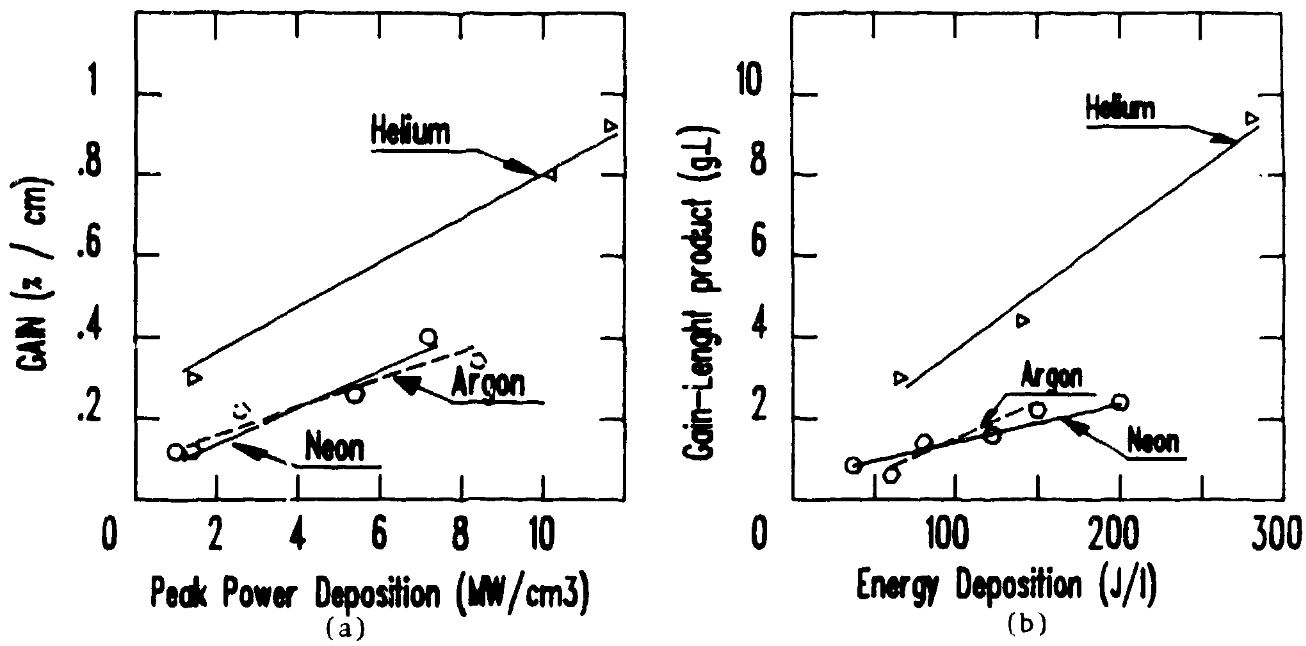

Figure 9. (a) peak gain versus peak-power deposition and (b) gain length product versus energy deposition are given for helium, neon, and argon buffers with 10 torr xenon and 5 torr fluorine partial pressures with no krypton.

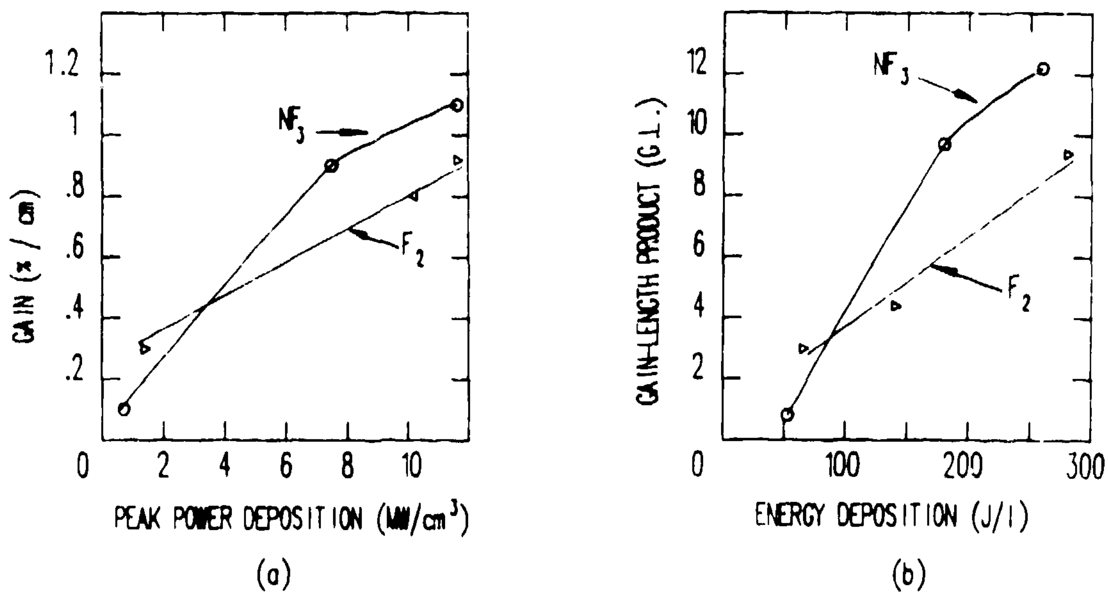

Figure 10. (a) peak gain versus peak-power deposition density and (b) gain-length product versus energy deposition in helium buffer at total pressure of 45 psia with 10 torr xenon partial pressure and 0 torr krypton pressure. Comparisons are made between NF_3 at 2 torr and F_2 at 5 torr partial pressure.

krypton partial pressure and for different buffer gases. Under the same gas composition the gain increases linearly with peak power deposition and the gain-length product increases linearly with energy deposited even though the gain is in the afterglow. Figure 10 shows similar measurements comparing different fluorine donors using helium buffer. The linear behavior for gain versus peak power deposition and gain-length product versus energy deposited is also observed under these conditions. There maybe some saturation effect using NF_3 as the fluorine donor but this may very well be within our experimental errors.

Discussion

Our observations show that both B and C state fluorescence takes place in the afterglow of the power deposition for power deposition times as longas 30 ns. The B and C state densities appear to be coupled tightly for all conditions we studied. The inclusion of krypton in the gas mix to increase the mixing rate between the states and to increase the absorption at the B-X transition wavelengths did little to improve the gain of the C-A transition. In the lasers using short pulse electron beam excitation, where the electron temperature is close to room temperature in the afterglow, increased mixing rate between the B and C states due to the presence of krypton tends to greatly favor the C state because at room temperature 90% of the population will be in the C state. The presence of electric fields in our discharges heat the electrons and keep them at temperatures where the B and C state populations are approximately equal. Thus, the inclusion of krypton is seen to increase the power deposition due to increase in the discharge impedance, but does not lead to improved gain because the kinetics decreased the upper state formation rate. Although it may be possible to match the power deposition to the discharge so accurately that no electric fields remain in the afterglow, we believe this to be an extremely difficult task.

The tight coupling between the B and C state has another detrimental consequence for strong C-A state lasing. Since

$$I_s = h\nu/\sigma_{st}\tau_Q,$$

τ_Q will be governed by the B state radiative lifetime rather than the C state in the absence of collisional quenching. This will result in an saturation intensity (I_s) nearly ten times higher than if the states are not tightly coupled, and it becomes that much more difficult to extract energy from the C state.

References

1. Y. Nachshon, F.K. Tittel, W.L. Wilson, Jr., and W.L. Nighan, "Efficient XeF(C-A) laser oscillation using electron-beam excitation," J. Appl. Phys., vol. 56, pp. 36-48 (1984)

2. W.L. Nighan, F.K. Tittel, W.L. Wilson, Jr., N. Nishida, Y. Zhu, and R. Sauerbrey, "Synthesis of rare gas-halide mixtures resulting in efficient XeF(C-A) laser oscillation," Appl. Phys. Lett., vol.45, pp.947-949 (1984)

3. H. Hoges and G. Marowsky, "Injection control of a discharge excited XeF (C-A) laser." IEEE J. Quant. Elec., vol.24, pp.827-832 (1988).

4. R.C. Hollins, D.L. Jordan, and J. Coutts, "Enhanced optical gain in a discharge excited XeF C-A medium," Optics Communications, vol. 58, pp.265-268 (1986)

5. R.C. Sze, T. Sakai, M. Sentis, M. Vannini, M. Maloney, and I. Bigio, "Time resolved fluorescence and gain studies in discharge devices on the C-A transition of XeF," Conference on Lasers and Electro-Optics, Baltimore (April 1989)